

RESEARCH

Open Access



Values of apparent diffusion coefficient in pancreatic cancer patients receiving neoadjuvant therapy

Yufei Chen¹, Chao Ma^{1,2*}, Panpan Yang², Kuanzheng Mao^{2,3}, Yisha Gao⁴, Luguang Chen², Zhen Wang², Yun Bian², Chengwei Shao² and Jianping Lu²

Abstract

Background To investigate the values of apparent diffusion coefficient (ADC) for the treatment response evaluation in pancreatic cancer (PC) patients receiving neoadjuvant therapy (NAT).

Methods This study included 103 NAT patients with histologically proven PC. ADC maps were generated using monoexponential diffusion-weighted imaging (b values: 50, 800 s/mm²). Tumors' minimum, maximum, and mean ADCs were measured and compared pre- and post-NAT. Variations in ADC values measured between pre- and post-NAT completion for NAT methods (chemotherapy, chemoradiotherapy), tumor locations (head/neck, body/tail), tumor regression grade (TRG) levels (0–2, 3), N stages (N0, N1/N2) and tumor resection margin status (R0, R1), were further analyzed.

Results The minimum, maximum, and mean ADC values all increased dramatically after NAT, rising from 23.4 to 25.4% (all $p < 0.001$): mean (average: 1.626×10^{-3} mm²/s vs. 1.315×10^{-3} mm²/s), minimum (median: 1.274×10^{-3} mm²/s vs. 1.034×10^{-3} mm²/s), and maximum (average: 1.981×10^{-3} mm²/s vs. 1.580×10^{-3} mm²/s). The ADCs between the subgroups of all the criteria under investigation did not differ significantly for the minimum, maximum, or mean values pre- or post-NAT ($P = 0.08$ to 1.00). In the patients with borderline resectable PC ($n = 47$), the rate of tumor size changes after NAT was correlated with the pre-NAT mean ADC values (Spearman's coefficient: 0.288, $P = 0.049$).

Conclusions The ADC values of PC increased significantly following NAT; however, the percentage increases failed to provide any predictive value for the resection margin status or TRG levels.

Keywords Apparent diffusion coefficient, Pancreatic cancer, Neoadjuvant therapy, Diffusion weighted imaging, Prediction

*Correspondence:

Chao Ma
mengqih@gmail.com

¹College of Electronic and Information Engineering, Tongji University, Shanghai, China

²Department of Radiology, Changhai Hospital of Shanghai, Naval Medical University, Changhai Road 168, Shanghai 200434, China

³School of Health Science and Engineering, University of Shanghai for Science and Technology, Shanghai, China

⁴Department of Pathology, Changhai Hospital of Shanghai, Naval Medical University, Shanghai, China



Background

Pancreatic cancer (PC) is a highly lethal ailment that causes over 460,000 fatalities each year [1], with a 5-year survival rate ranging from 2 to 12% [2, 3]. As the annual mortality rate increases, PC-related fatalities may be the second leading cause of death in the United States by 2030 [4]. A significant proportion of patients are identified with distant metastasis or local tumor progression rather than timely surgical resection due to the absence of an efficacious screening method for PC and the asymptomatic or atypical symptoms observed during early phases of PC. Only 10–15% of patients meet the criteria to undergo curative resection [5]. Furthermore, the development of novel treatment strategies for PC is imperative, alongside its early detection.

A recently developed treatment strategy for PC [6–11], neoadjuvant therapy (NAT) decreases tumor stage, post-operative recurrence, and metastasis. This improves the number of patients who are able to undergo surgery for locally advanced and borderline resectable PC, as well as increases the percentage of tumors that are removed via R0 resection. Both CT and MRI yield comparable results for PC staging and diagnosis [12]. In clinical applications, quantitative MRI has emerged as an essential tool, not only aiding radiologists in their clinical diagnoses but also assisting in the elimination of diagnostic subjectivity and furnishing standardized, calibrated parameters to account for system variations [13]. Clinical practice frequently employs apparent diffusion coefficient (ADC) derived from diffusion-weighted imaging (DWI) [14, 15] techniques to quantify the diffusion of water molecules through tissues. Standard criteria for the collection and analysis of DWI have been suggested [16–20] in order to expand the potential of ADC to be utilized in a variety of organs. The characteristics of certain tissues, including cellularity, vascularity, and the Ki-67 index, have been identified to correlate with variations in the ADC values of pancreatic tumors [21–23]. ADC has been used to evaluate the effects of NAT on PC patients [24]. There is ongoing debate regarding the effects of ADC measurements in PC patients undergoing NAT therapy [25–30]. ADC values are substantially impacted by alterations in the tissue components of PC following NAT, including necrosis, edema, inflammation, fibrosis, and the elimination of tumor cells and adjacent tissue. In light of the limited sample size observed in previous investigations [25–30], it is necessary to clarify the values of ADC on PC patients with NAT, so as to augment the accuracy of quantitative DWI for assessing treatment response. The objective of this study was to assess the utility of ADC in predicting prognostic parameters such as R0 resectability or tumor regression grade (TRG) levels among patients with PC, and to evaluate the value of ADC for the treatment response evaluation of PC patients with NAT.

Methods

Patients

The retrospective was granted approval by the Biomedical Research Ethics Committee of our institution. Between April 2019 and December 2021, 1752 patients underwent contrast-enhanced MRI or CT and received pancreatic tumor surgery. A total of 125 patients (72 men, 53 women; mean age, 60.6 ± 8.5 years) who underwent surgical excision of malignancies and were given NAT. Among these patients, 109 patients underwent contrast-enhanced MRI examinations prior to NAT, and 115 individuals underwent contrast-enhanced MRI examinations after the completion of NAT. Finally, this study included 103 individuals who underwent MRIs in both the pre-NAT and post-NAT groups (Fig. 1). Out of the 103 cases, 39 patients underwent twice MRI examinations with the same scanner, one before and one after the NAT was concluded.

MRI

All patients underwent MRI examinations utilizing pancreatic protocols on 1.5-T or 3-T MRI systems (Signa HDxt and Discovery MR750, GE Healthcare, Milwaukee, USA; MAGNETOM Skyra and Avanto, Siemens, Erlangen, Germany), which include T1-weighted imaging (T1WI) with two echoes and water-fat Dixon reconstruction, contrast-enhanced T1WI (contrast agent, 0.1–0.15 mmol/kg; rate, 2.0–3.0 ml/s), DWI and magnetic resonance cholangiopancreatography (MRCP). DWI employed a single-shot free-breathing echo-planar-imaging sequence with three orthogonal diffusion gradients. Table 1 provides a summary of the DWI parameters utilized by MRI scanners at present. Tumor diameters were measured using the response evaluation criteria in solid tumors (RECIST) 1.1 criteria in conjunction with MRI.

ADC measurements

The ADC maps were generated by utilizing a monoexponential model DWI (b-values: 50 and 800 s/mm²). By delineating one elliptical or circular region of interest (ROI) on the solid portion of the tumor for each patient (Figs. 2 and 3), with caution to exclude cystic lesions and dilated pancreatic duct by the collaboration of two measurers, who calculated the mean, minimum, and maximum ADC values for every patient both before and after NAT. A radiologist (12 years' experience in abdominal MRI) and an MRI physicist (13 years' experience in abdominal MRI) determined the ADCs utilizing Image J (v1.8.0; National Institutes of Health, Bethesda, USA) and RadiAnt DICOM viewer (v2021.1; Medixant, Poznan, Poland).

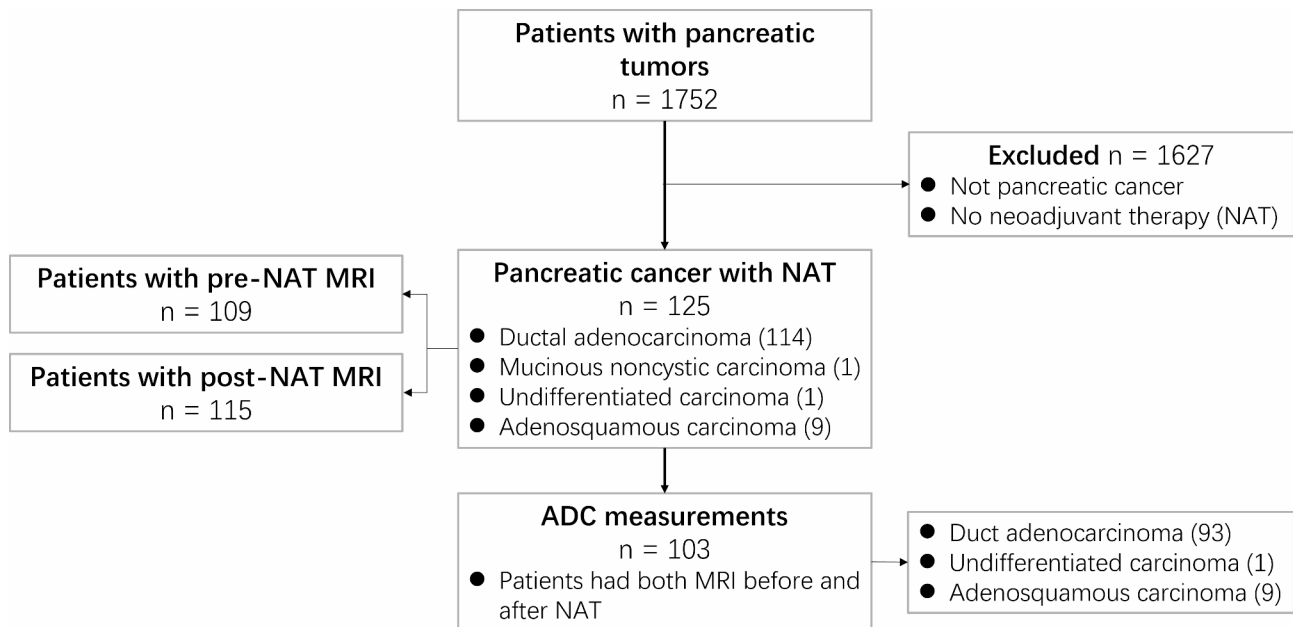


Fig. 1 Flow chart of the patient selection process

Table 1 The diffusion weighted imaging parameters for the MRI scanners used in this study

MRI Scanners	Field strength (tesla)	Time of repetition (ms)	Time of echo (ms)	Field of view (mm ²)	b values (s/mm ²)	Matrix	Slice/gap Thickness (mm)	Number of slices
GE Signa HDxt	3	3000	59.2	380*304	0, 50, 800	128×128	6/1	26
GE Discovery MR750	3	3329	76.4	360*288	50, 800	128×128	6/1	30
Siemens MAGNETOM Skyra	3	4800	48	380*308	50, 800	128×104	6/1.2	26
Siemens MAGNETOM Avanto	1.5	4000	75	380*285	50, 800	128×96	5/1.5	25

59, 91, 31 and 25 examinations were performed by each MRI scanners, respectively

Pathological analysis

The macroscopic description, specimen specifications, morphological description, margins and neighbors, lymph node metastasis, diagnosis, TRG, and other pertinent information were documented in the structured pathological reports for NAT of PC at our hospital. TRG is classified into four phases (Grades 0 to 3) by the College of American Pathologists (CAP) grading system, which is determined by the proportion of residual tumor cells to stroma. Grade 0 indicates complete response to PC with no surviving tumor cells, Grade 1 indicates the presence of a solitary or small number of focal residual tumor cells; Grade 2 indicates the presence of focal residual tumor cells accompanied by interstitial fibrosis; and Grade 3 indicates that the NAT was ineffective and a considerable number of tumor cells persisted. R0 and R1 were ascertained in the absence of tumor cell infiltration within a 1 mm margin of the resection. Prior to the issuance of final pathology reports, pathological images were analyzed by a minimum of two pathologists. The Ki-67 labeling index represents the percentage of nuclei positively stained among the whole tumor cells.

Statistical analysis

MedCalc (version 13.0.0.0, MedCalc Software, Ostend, Belgium) was utilized for statistical analysis. Normality assumptions of ADCs were assessed using the Kolmogorov-Smirnov test. Normal distribution data are expressed as mean±standard deviation (range), and non-normally distributed data are expressed as median (range). Wilcoxon tests or T-tests were used to examine potential differences in the measured ADC values (mean, minimum, and maximum) between samples collected before and after NAT. NAT methods (chemotherapy, chemoradiation), tumor locations (head/neck, body/tail), TRG levels (0–2, 3), N stages (N0, N1/N2), and tumor resection margin status (R0, R1) were considered when comparing the mean, minimum, and maximum ADCs between the two groups before and after NAT using Mann-Whitney or independent samples T-tests. The gross, pre-NAT, and post-NAT MRI tumor sizes were compared using the Friedman test with post hoc analysis. The correlation between the pre- and post-NAT ADCs, the rate of ADC changes post-NAT, and the rate of tumor size changes post-NAT were examined using Spearman

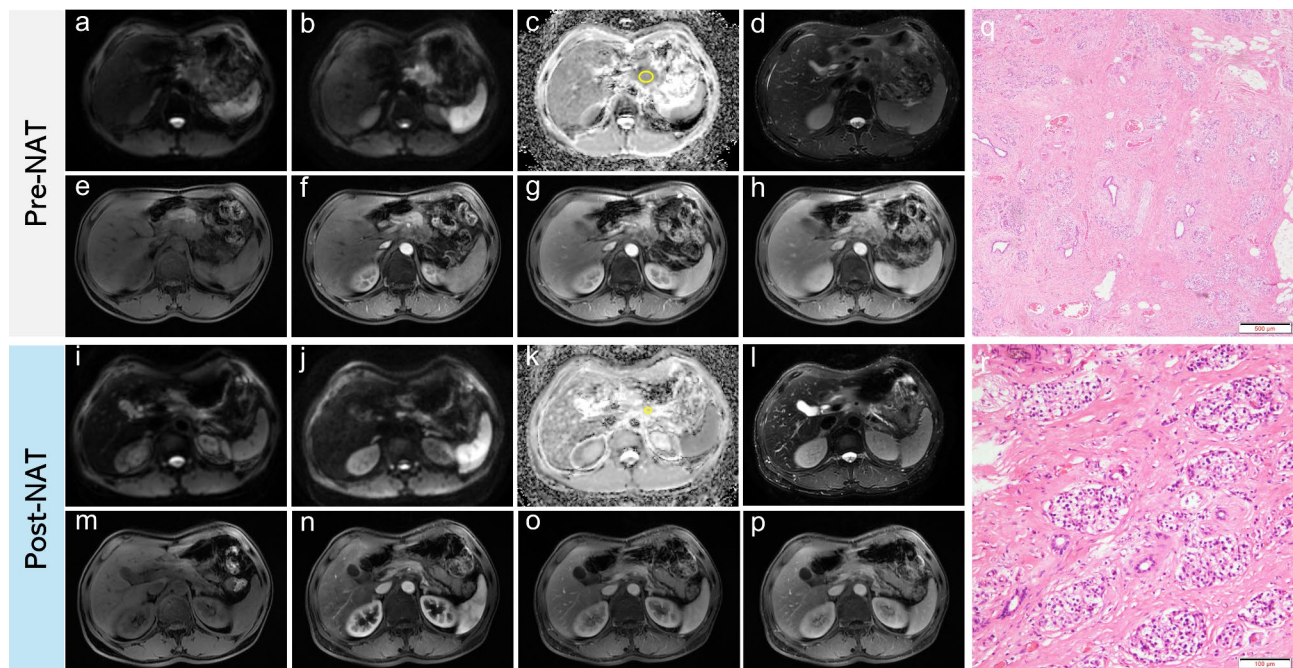


Fig. 2 Representative MRI images and apparent diffusion coefficient (ADC) measurements of pancreatic cancer with tumor regression grade 0 before and after neoadjuvant therapy (NAT). MRI scans taken pre- and post-NAT are shown in (a–h) and (i–p). Figures (a, i) and (b, j) are diffusion-weighted images with b value of 50 and 800 s/mm², respectively; (c, k) ADC maps; (d, l) T2-weighted images; (e, m) Pre-contrast water images of the DIXON VIBE; (f, n) Arterial phase T1WI; (g, o) Venous-phase T1WI; (h, p) Delayed-phases T1-weighted images; (q) H&E, magnification×40 and (r) H&E, magnification ×200. On the ADC maps, a rounded or oval-shaped region of interest (ROI) is drawn within the solid tumor areas for ADC measurements. The tumor's mean, minimum, and maximum ADC values can be determined via an ROI (Pre-NAT: ROI, 280.8 mm²; mean: 1.036×10^{-3} mm²/s; minimum: 0.761×10^{-3} mm²/s; maximum: 1.287×10^{-3} mm²/s; Post-NAT: ROI, 64.5 mm²; mean: 2.009×10^{-3} mm²/s; minimum: 1.758×10^{-3} mm²/s; maximum: 2.319×10^{-3} mm²/s). (Yellow ROI examples in figures c and k)

correlation analyses. Furthermore, we also carried out correlation analyses to examine the correlations between ADC values and Ki-67 or the tumor grade. The threshold for statistical significance was established as $P < 0.05$.

Results

Patient characteristics

Table 2 provides a summary of the clinical characteristics of the 103 patients. The mean age of the 61 males and 42 females was 59.7 ± 8.6 years (range: 33–76). Of the total pancreatic lesions detected, 52.4% (54 of 103) were located in the head/neck area. Histological analyses identified lymph node metastases in 50% (51 of 102) of patients, excluding one individual who did not undergo peripancreatic lymphadenectomy. At the time of tumor resection, 74.8% (77 of 103) of the cases included in this study had R0 margin status. The median tumor size as determined by pre-NAT, preoperative MRI, and pathological measurements was 30.0 mm (range, 8.2 to 89 mm), 20.0 mm (range, 0 to 56.6 mm), and 28.0 mm (range, 5 to 75 mm), respectively. Among the three groups, PC had the smallest preoperative median MRI size. Ki-67 were recorded in 97 patients, with a median of 30% (range, 0 to 90%).

ADC measurements pre- and post-NAT

Subsequent to NAT, the mean ADC of tumors increased by 23.3%, the minimum ADC increased by 25.4%, and the maximum ADC increased by approximately 23.4% (Table 3). Pre- or post-NAT, the difference between the subgroups of all the investigated factors was not significant ($P = 0.085$ to 0.999) for the ADC measurements of PC on both the two groups in factors such as NAT methods, tumor locations, TRG levels, N stages, and resection margin status. In particular, pre- or post-NAT, the difference among the groups of TRG (G0/G1, G2, G3), was also not significant for the ADC_{mean}, ADC_{max} and ADC_{min} with P values ranging from 0.070 to 0.719.

Further analysis revealed significant fluctuations in the ADC values, encompassing the minimum, mean, and maximum, when longitudinal comparisons of ADC measurements were conducted between the subgroups of all parameters examined before and after NAT (all $P < 0.01$). There was no correlation observed between the rate of change in tumor size and the pre-NAT ADC values or the rate of change in any of the three categories (mean, minimum, and maximum) following NAT completion ($P = 0.237$ to 0.967).

Furthermore, the analyses of ADC values before and after NAT treatment for the 39 patients who underwent

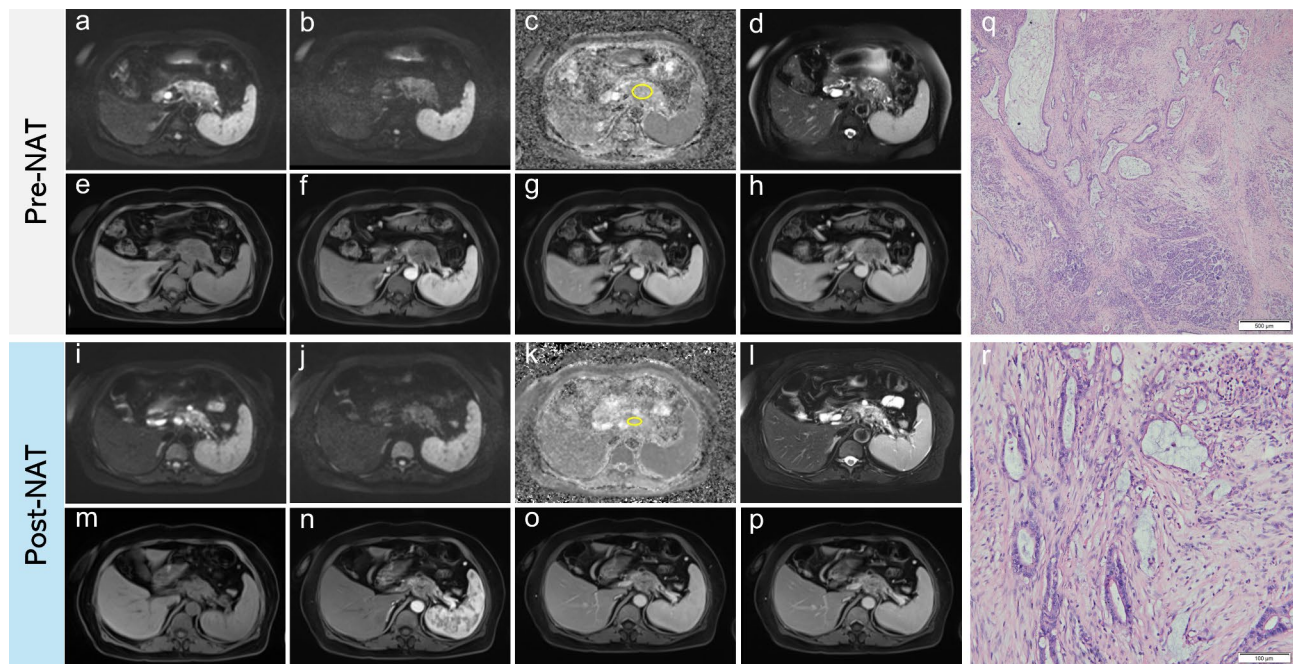


Fig. 3 Representative MRI images and apparent diffusion coefficient (ADC) measurements of pancreatic cancer with tumor regression grade 3 pre- and post-neoadjuvant therapy (NAT). MRI scans taken pre- and post-NAT are shown in (a–h) and (i–p). Figures (a, i) and (b, j) are diffusion-weighted images with b value of 50 and 800 s/mm², respectively; (c, k) ADC maps; (d, l) T2-weighted images; (e, m) Pre-contrast water images of the DIXON VIBE; (f, n) Arterial phase T1WI; (g, o) Venous-phase T1WI; (h, p) Delayed-phases T1-weighted images; (q) H&E, magnification×40 and (r) H&E, magnification ×200. On the ADC maps, a rounded or oval-shaped region of interest (ROI) is drawn within the solid tumor areas for ADC measurements. The tumor's mean, minimum, and maximum ADC values can be determined via an ROI (Pre-NAT: ROI, 581.7 mm²; mean: 1.371×10^{-3} mm²/s; minimum: 0.894×10^{-3} mm²/s; maximum: 1.905×10^{-3} mm²/s; Post-NAT: ROI, 202.7 mm²; mean: 1.740×10^{-3} mm²/s; minimum: 1.443×10^{-3} mm²/s; maximum: 2.164×10^{-3} mm²/s). (Yellow ROI examples in figures c and k)

MRI scans on the identical MRI scanners prior to and following NAT treatment yielded comparable outcomes to those observed in the 103 cases.

After NAT, the Ki-67 of patients with TRG levels of 0–2 (median, 20%; range, 0 to 90%) was significantly lower than that of patients with TRG level TRG 3 (median, 30%; range, 3–90%) with *P* value of 0.018. There was no correlation between ADC values (mean, minimum, and maximum) and Ki-67 (*P*=0.102 to 0.789) or TRG levels (*P*=0.090 to 0.973) pre- or post-NAT (Table 4).

ADC measurements of borderline resectable PC

In this study, 47 patients with PC that was borderline resectable participated. Following NAT, the mean, minimum, and maximum ADC values of tumors increased by roughly 21.8%, 22.7%, and 21.6%, respectively. Before or after NAT, there was no significant difference (*P*=0.077 to 0.956) between the subgroups of all tested parameters for the ADC measurements of PC on TRG levels (0–2, 3) and resection margin status (R0, R1). There was a correlation between the rate of tumor size variations following NAT and the mean ADC values prior to NAT (Spearman's coefficient: 0.288, *P*=0.049).

Discussion

To reduce the variability of ADC data, this study applies the identical combination (50 and 800 s/mm²) for ADC calculation across to all MRI systems. A multi-b-value DWI study utilizing six models suggests that DWI can be employed to examine changes in PC both before and after NAT [31]. The performance of the quantitative parameter of ADC changes before and after NAT was superior to that of the parameter's own repeatability. Following NAT, the minimum, maximum, and mean ADCs for PC patients increased significantly, as shown in the present study; however, there was no significant difference in the percentage increases for R0 resectability or TRG levels. The mean tumor ADC of the 103 patients prior to NAT was 1.31×10^{-3} mm²/s, which was within the range of ADCs associated with PC [32]. The average ADC values of the tumors from 103 patients increased by about 25.4% to 1.626×10^{-3} mm²/s subsequent to NAT. The elimination of PC cells subsequent to NAT may facilitate water molecule diffusion and contribute to the increased ADC values.

Prior investigations concerning the impact of ADC on the prediction of NAT's effectiveness for PC have produced controversial findings. An association between the pathological response of the tumor and the baseline

Table 2 Characteristics of the enrolled 103 patients with pancreatic cancer

Mean age \pm SD, years (range)	59.7 \pm 8.6 (33–76)
Gender, n (%)	
Male	61 (59.2%)
Female	42 (40.8%)
Location in pancreas, n (%)	
Head/neck	54 (52.4%)
Body/tail	49 (47.6%)
Resectability of pancreatic cancer, n (%)	
Resectable	43 (41.8%)
Borderline resectable	47 (45.6%)
Locally advanced	13 (12.6%)
Histopathologic features of mass, n (%)	
Ductal adenocarcinoma	93 (90.3%)
Adenosquamous carcinoma	9 (8.7%)
Undifferentiated carcinoma	1 (1.0%)
Tumor resection margin status, n (%)	
R0	77 (74.8%)
R1	26 (25.2%)
Year of surgery	2019–2021
N stage, n (%)	
NX	1 (1.0%)
N0	51 (49.5%)
N1	40 (38.8%)
N2	11 (10.7%)
Tumor regression grade, n (%)*	
0	2 (1.9%)
1	9 (8.8%)
2	59 (57.3%)
3	33 (32.0%)

SD: standard deviation

*Grading system of the College of American Pathologists

mean ADC value was identified by Cuneo et al. [24] through the analysis of DWI images from seven patients who had resectable PC prior to NAT. In contrast to the non-responding patient group, the responding patient group exhibited a higher pre-NAT ADC baseline value.

Chan et al. discovered, using a sample of thirteen cases, that ADC increased in 54% of instances after NAT, and in 95% of those instances, it increased by more than 10% [25]. Using genetically modified rodents as models for PC NAT, Trajkovic-Arsic et al. [33] discovered that ADC can be used to predict the early NAT response of PC. The study also compared the mean ADC before and after NAT in six PC patients and discovered that the cases with the greatest decrease in tumor size had the greatest ADC increases after NAT. The study conducted by Zimmermann et al. [28] examined 25 patients and found that the average ADC values were $1.32 \times 10^{-3} \text{ mm}^2/\text{s}$ prior to NAT completion and $1.43 \times 10^{-3} \text{ mm}^2/\text{s}$ subsequent to NAT completion [28]. The distinction between the two categories was not readily apparent. Multiple studies [25, 27, 30, 34] indicate that the average ADC for PC is considerably greater after NAT than it was prior to NAT. The findings corroborate our assertions. Following NAT, there is a possibility of decreased tumor cell density and stromal reorganization, both of which could impact the ability of water molecules to diffuse across the tissue and facilitate the utilization of DWI to identify alterations in ADC values. Our findings suggest that ADC effectively captures the changes that occur in PC following NAT, despite the non-uniformity of the NAT techniques employed in the patients. Further research will be guided by these noteworthy findings.

Studies on a variety of tumors have shown that ADC values can be used to predict pathological features [35–37]. Ki-67 is an indicator of cell proliferation and could be used for the evaluation of tumors. In the liver metastases from both breast and colorectal cancers, a significant correlation was observed between ADC values and Ki-67 indices. Conversely, in the case of pancreatic cancer metastases, no substantial correlations were detected [38]. Ki-67 demonstrates a significant correlation with ADC values in primary central nervous system lymphoma [39]. In meningioma, the authors observed an

Table 3 Comparisons of ADC measurements of pancreatic cancer ($n = 103$) before and after neoadjuvant therapy (NAT)

ADC measurements	Pre-NAT	Post-NAT
ROI (mm^2)		
Median (Interquartile range)	156.3 (115.0–233.3)	117.8 (88.8–150.0)
P value	< 0.001	
Minimum ($\times 10^{-3} \text{ mm}^2/\text{s}$)		
Median (Interquartile range)	1.034 (0.935–1.191)	1.274 (1.106–1.451)
P value	< 0.001	
Mean ($\times 10^{-3} \text{ mm}^2/\text{s}$)		
Average \pm SD (Range)	1.315 \pm 0.195 (0.903–1.917)	1.626 \pm 0.291 (1.054–2.400)
P value	< 0.001	
Maximum ($\times 10^{-3} \text{ mm}^2/\text{s}$)		
Average \pm SD (Range)	1.580 \pm 0.232 (1.092–2.387)	1.981 \pm 0.384 (1.217–3.137)
P value	< 0.001	

ADC: apparent diffusion coefficient; SD: standard deviation

Table 4 Correlations between ADC values and the Ki67 index, as well as tumor grade before and after neoadjuvant therapy (NAT)

	Parameters	Ki-67(%)		TRG levels	
		Correlation coefficient <i>r</i> (95% CI)	<i>P</i>	Correlation coefficient <i>r</i> (95% CI)	<i>P</i>
Pre-NAT	ADC _{min}	-0.027 (-0.226 to 0.173)	0.789	0.003 (-0.197 to 0.190)	0.973
	ADC _{mean}	-0.055 (-0.252 to 0.146)	0.593	-0.029 (-0.221 to 0.165)	0.771
	ADC _{max}	-0.081 (-0.276 to 0.120)	0.429	-0.021 (-0.214 to 0.173)	0.831
Post-NAT	ADC _{min}	-0.167 (-0.355 to 0.033)	0.102	0.133 (-0.063 to 0.318)	0.182
	ADC _{mean}	-0.129 (-0.320 to 0.072)	0.208	0.168 (-0.026 to 0.350)	0.090
	ADC _{max}	-0.088 (-0.283 to 0.113)	0.390	0.106 (-0.089 to 0.294)	0.286

CI: Confidence interval

inverse correlation between Ki-67 and both ADC_{mean} and ADC_{max}, while no significant correlation was found with ADC_{min} [40]. Surov et al. noted that ADC values are not predictive of molecular subtypes or lymph node metastases in invasive breast cancer. However, they did find a weak correlation between ADC and the expression levels of Ki-67 [41, 42]. For the pancreatic tumors, a negative correlation between pathological features such as tumor cellularity and Ki-67 and ADC values of pancreatic neuroendocrine tumors [23, 43]. Xie et al. found the ADCs of PC was not significantly correlated with Ki-67 [22]. In the current study, we also found that the ADCs of PC before and after NAT were not correlated with Ki-67 and TRG levels. Consequently, ADC values are not suitable as a proliferation biomarker for PC.

Two critical clinical indicators of NAT are the TRG levels of PC and the state of the resection margin. In this study, we analyzed the variations in ADC among PC patients with NAT, stratified by resection margin status and TRG levels, including the mean, minimum, and maximum ADC values. Before or after NAT, there was no discernible difference in any of the examined parameters between the subgroups. Pre- and post-NAT ADC measurements were unable to predict tumor treatment response, including margin status and TRG levels of PC, according to our findings. kada et al. [26] identified the pre-NAT ADC value as a predictor of R0 curability in patients with borderline resectable PC in a retrospective study. However, the authors of another prospective study found that the post-treatment ADC value may serve as a predictor of R0 resectability in patients with borderline resectable PC [27]. Contradictory findings may be attributable to the varied case sources and tiny sample sizes utilized in the studies. The grading of TRGs is predominantly determined by the existence of interstitial fibrosis induced by treatment and damaged tumor cells. Pancreatic cancer cells are extensively distributed and proliferate haphazardly in this investigation. In general, tumor cells are distributed across an extensive array of proliferative stroma, with a particular concentration in the vicinity of the tumor. Interstitial fibrosis induced by NAT is comparable in appearance to fibroproliferative stroma linked to PC and fibrosis resulting from chronic

pancreatitis. Consequently, the grading of TRG may be imprecise and subjective. Conversely, clinical pathology is subject to certain constraints on account of the utilization of minuscule tissue samples. Additional analysis of 47 patients with equivocal resectable PC in this study revealed no differences in pre-treatment or post-treatment ADC measurements or TRG levels (0–2, 3) between the R0 and R1 groups.

The preoperative MRI tumor sizes subsequent to NAT were notably reduced in comparison to the pre-NAT MRI tumor sizes and the pathological size of PC (both $P < 0.001$), with a median underestimation of tumor size was approximately 10 mm and 8 mm, respectively. In prior publications, we delineated various rationales for the incongruity between the pathology findings and the imaging sizes of the tumors [44–46]. The present study examined the correlation between the pre-NAT mean ADC values and the rate of variations in tumor size for the borderline resectable PC. Hence, the mean ADCs prior to NAT could potentially serve as a metric for assessing the effectiveness of NAT in the treatment of pancreatic cancer [30], although its value requires additional verification.

There were several limitations to this investigation. First, there were variations in the neoadjuvant techniques utilized in this study. For example, albumin-bound paclitaxel, gemcitabine, FOLFIRINOX, and mFOLFIRINOX have all been utilized in chemotherapy. Due to the imperfection of the post-NAT staging system and the evolution of NAT protocols and treatment recommendations in recent years, it is difficult to manage PC patients in clinical practice [47]. Second, although previous research has shown that employing multiple b values can lead to more precise ADC value measurements [48], in our clinical context of pancreatic MRI, ADC maps were constructed using DWI with only two b values in order to balance scanning time. Third, PC tumor cells are often distributed across a diverse array of stroma, particularly in the immediate vicinity of the tumor. It is challenging to describe the contour of the tumor, particularly after NAT, and imaging evaluation typically underestimates the number of tumor cells dispersed throughout the tumor [10]. In this investigation, the ADC values were therefore

measured using the solid sample ROI method [49, 50]. Prior research has extensively investigated the impact of ROI approaches, including whole-volume, single-slice, and solid tumor samples, on the measurements of ADC values [49, 50]. However, we refrained from evaluating this particular influence.

Conclusions

Increasing percentage values did not predict the R0 resectability and TRG levels in PC patients, despite the fact that the minimum, maximum, and mean ADC values all increased substantially after NAT for the examinations done in the routine praxis.

Abbreviations

ADC	Apparent diffusion coefficients
CAP	College of American pathologists
CT	Computed tomography
DICOM	Digital imaging and communications in medicine
DWI	Diffusion-weighted imaging
MRCP	Magnetic resonance cholangiopancreatography
MRI	Magnetic resonance imaging
NAT	Neoadjuvant therapy
PC	Pancreatic cancer
RECIST	Response evaluation criteria in solid tumors
ROI	Regions of interest
T1WI	T1-weighted imaging
TRG	Tumor regression grade

Author contributions

C.Y., Y.P., M.K., G.Y., W.Z., L.C., M.C. and B.Y. performed the majority of experiments, made substantial contributions to the data analysis and interpretation, and wrote the manuscript draft; M.C., C.Y., S.C. and L.J. participated in the design of the study and made substantial contribution to data analysis; M.C. made substantial contributions to the study conception and design, critically revised the manuscript draft for important intellectual content, and gave final approval of the version to be published; all the authors read and approved the final manuscript.

Funding

This work was supported by the National Natural Science Foundation of China [82073307, 62173252]; 234 Platform Discipline Consolidation Foundation Project of Changhai Hospital [2020YPT001]; Shanghai Science and Technology Innovation Action Plan Medical Innovation Research Project [20Y11912500].

Data availability

The research dataset for the current study is available from the corresponding author upon reasonable request.

Declarations

Ethics approval and consent to participate

This study was performed in line with the principles of the Declaration of Helsinki. Approval was granted by the Ethics Committee Changhai Hospital of Shanghai. Signed written informed consent was obtained from all participants.

Consent for publication

Not applicable.

Competing interests

The authors declare no competing interests.

Received: 24 January 2024 / Accepted: 11 September 2024

Published online: 18 September 2024

References

- Sung H, Ferlay J, Siegel RL, Laversanne M, Soerjomataram I, Jemal A, et al. Global cancer statistics 2020: GLOBOCAN estimates of incidence and mortality worldwide for 36 cancers in 185 countries. *CA Cancer J Clin*. 2021;71(3):209–49.
- Siegel RL, Miller KD, Wagle NS, Jemal A. Cancer statistics, 2023. *CA Cancer J Clin*. 2023;73(1):17–48.
- McGuigan A, Kelly P, Turkington RC, Jones C, Coleman HG, McCain RS. Pancreatic cancer: a review of clinical diagnosis, epidemiology, treatment and outcomes. *World J Gastroenterol*. 2018;24(43):4846–61.
- Saad AM, Turk T, Al-Husseini MJ, Abdel-Rahman O. Trends in pancreatic adenocarcinoma incidence and mortality in the United States in the last four decades; a SEER-based study. *BMC Cancer*. 2018;18(1):688.
- Park W, Chawla A, O'Reilly EM. Pancreat cancer: a review. *JAMA*. 2021;326(9):851–62.
- Tempero MA, Malafa MP, Al-Hawary M, Behrman SW, Benson AB, Cardin DB, et al. Pancreatic adenocarcinoma, version 2.2021, NCCN clinical practice guidelines in oncology. *J Natl Compr Canc Netw*. 2021;19(4):439–57.
- Kulkarni NM, Soloff EV, Tolat PP, Sangster GP, Fleming JB, Brook OR, et al. White paper on pancreatic ductal adenocarcinoma from society of abdominal radiology's disease-focused panel for pancreatic ductal adenocarcinoma: part I, AJCC staging system, NCCN guidelines, and borderline resectable disease. *Abdom Radiol (NY)*. 2020;45(3):716–28.
- Gugenheim J, Crovetto A, Petrucciani N. Neoadjuvant therapy for pancreatic cancer. *Updates Surg*. 2022;74(1):35–42.
- Versteijne E, van Dam JL, Suker M, Janssen QP, Groothuis K, Akkermans-Vogelaar JM, et al. Neoadjuvant chemoradiotherapy versus upfront surgery for resectable and borderline resectable pancreatic cancer: long-term results of the Dutch randomized PREOPANC trial. *J Clin Oncol*. 2022;40(11):1220–30.
- Soloff EV, Al-Hawary MM, Desser TS, Fishman EK, Minter RM, Zins M. Imaging assessment of pancreatic cancer resectability after neoadjuvant therapy: *AJR* expert panel narrative review. *AJR Am J Roentgenol*. 2022;218(4):570–81.
- Heinrich S, Lang H. Neoadjuvant therapy of pancreatic cancer: definitions and benefits. *Int J Mol Sci*. 2017;18(8):1622.
- Treadwell JR, Zafar HM, Mitchell MD, Tipton K, Teitelbaum U, Jue J. Imaging tests for the diagnosis and staging of pancreatic adenocarcinoma: a meta-analysis. *Pancreas*. 2016;45(6):789–95.
- Shukla-Dave A, Obuchowski NA, Chenevert TL, Jambawalikar S, Schwartz LH, Malayarenko D, et al. Quantitative imaging biomarkers alliance (QIBA) recommendations for improved precision of DWI and DCE-MRI derived biomarkers in multicenter oncology trials. *J Magn Reson Imaging*. 2019;49(7):e101–21.
- Taouli B, Beer AJ, Chenevert T, Collins D, Lehman C, Matos C, et al. Diffusion-weighted imaging outside the brain: consensus statement from an ISMRM-sponsored workshop. *J Magn Reson Imaging*. 2016;44(3):521–40.
- Padhani AR, Liu G, Koh DM, Chenevert TL, Thoeny HC, Takahara T, et al. Diffusion-weighted magnetic resonance imaging as a cancer biomarker: consensus and recommendations. *Neoplasia*. 2009;11(2):102–25.
- Ni P, Lin Y, Zhong Q, Chen Z, Sandrasegaran K, Lin C. Technical advancements and protocol optimization of diffusion-weighted imaging (DWI) in liver. *Abdom Radiol*. 2016;41(1):189–202.
- Baltzer P, Mann RM, Lima M, Sigmund EE, Clauser P, Gilbert FJ, et al. EUSOBI international breast diffusion-weighted imaging working group. Diffusion-weighted imaging of the breast—a consensus and mission statement from the EUSOBI International breast diffusion-weighted imaging working group. *Eur Radiol*. 2020;30(3):1436–50.
- Ljimini A, Caroli A, Laustsen C, Francis S, Mendichovszky IA, Bane O, et al. Consensus-based technical recommendations for clinical translation of renal diffusion-weighted MRI. *MAGMA*. 2020;33(1):177–95.
- Beets-Tan RGH, Lambregts DMJ, Maas M, Bipat S, Barbaro B, Curvo-Semedo L, et al. Magnetic resonance imaging for clinical management of rectal cancer: updated recommendations from the 2016 European Society of Gastrointestinal and Abdominal Radiology (ESGAR) consensus meeting. *Eur Radiol*. 2018;28(4):1465–75.
- Barnes A, Alonzi R, Blackledge M, Charles-Edwards G, Collins DJ, Cook G, et al. UK quantitative WB-DWI technical workgroup: consensus meeting recommendations on optimisation, quality control, processing and analysis of quantitative whole-body diffusion-weighted imaging for cancer. *Br J Radiol*. 2018;91(1081):20170577.
- Nissan N. Modifications of pancreatic diffusion MRI by tissue characteristics: what are we weighting for? *NMR Biomed*. 2017;30(8):e3728.
- Xie P, Liu K, Peng W, Zhou Z. The correlation between diffusion-weighted imaging at 3.0-T magnetic resonance imaging and histopathology

- for pancreatic ductal adenocarcinoma. *J Comput Assist Tomogr.* 2015;39(5):697–701.
23. Wang Y, Chen ZE, Yaghmai V, Nikolaidis P, McCarthy RJ, Merrick L, Miller FH. Diffusion-weighted MR imaging in pancreatic endocrine tumors correlated with histopathologic characteristics. *J Magn Reson Imaging.* 2011;33(5):1071–9.
 24. Cuneo KC, Chenevert TL, Ben-Josef E, Feng MU, Greenson JK, Hussain HK, et al. A pilot study of diffusion-weighted MRI in patients undergoing neoadjuvant chemoradiation for pancreatic cancer. *Transl Oncol.* 2014;7(5):644–9.
 25. Chan E, Arlinghaus LR, Cardin DB, Goff L, Berlin JD, Parikh A, et al. Phase I trial of vorinostat added to chemoradiation with capecitabine in pancreatic cancer. *Radiother Oncol.* 2016;119(2):312–8.
 26. Okada KI, Hirono S, Kawai M, Miyazawa M, Shimizu A, Kitahata Y, et al. Value of apparent diffusion coefficient prior to neoadjuvant therapy is a predictor of histologic response in patients with borderline resectable pancreatic carcinoma. *J Hepatobiliary Pancreat Sci.* 2017;24(3):161–8.
 27. Okada KI, Kawai M, Hirono S, Kojima F, Tanioka K, Terada M, et al. Diffusion-weighted MRI predicts the histologic response for neoadjuvant therapy in patients with pancreatic cancer: a prospective study (DIFFERENT trial). *Langenbecks Arch Surg.* 2020;405(1):23–33.
 28. Zimmermann C, Distler M, Jentsch C, Blum S, Folprecht G, Zöphel K, et al. Evaluation of response using FDG-PET/CT and diffusion weighted MRI after radiochemotherapy of pancreatic cancer: a non-randomized, monocentric phase II clinical trial-PaCa-DD-041 (Eudra-CT 2009-011968-11). *Strahlenther Onkol.* 2021;197(1):19–26.
 29. Kang JH, Lee SS, Kim JH, Byun JH, Kim HJ, Yoo C, et al. Multiparametric MRI for prediction of treatment response to neoadjuvant FOLFIRINOX therapy in borderline resectable or locally advanced pancreatic cancer. *Eur Radiol.* 2021;31(2):864–74.
 30. Hussien N, Hussien RS, Saad DHA, El Kassas M, Elkhatib WF, Ezz El Din M. The role of MRI pancreatic protocol in assessing response to neoadjuvant therapy for patients with borderline resectable pancreatic cancer. *Front Oncol.* 2022;13:11796317.
 31. Klaassen R, Gurney-Champion OJ, Engelbrecht MRW, Stoker J, Wilmink JW, Besselink MG, et al. Evaluation of six diffusion-weighted MRI models for assessing effects of neoadjuvant chemoradiation in pancreatic cancer patients. *Int J Radiat Oncol Biol Phys.* 2018;102(4):1052–62.
 32. Barral M, Taouli B, Guiu B, Koh DM, Luciani A, Manfredi R, et al. Diffusion-weighted MR imaging of the pancreas: current status and recommendations. *Radiology.* 2015;274(1):45–63.
 33. Trajkovic-Arsic M, Heid I, Steiger K, Gupta A, Fingerle A, Wörner C, et al. Apparent diffusion coefficient (ADC) predicts therapy response in pancreatic ductal adenocarcinoma. *Sci Rep.* 2017;7(1):17038.
 34. Dalah E, Erickson B, Oshima K, Schott D, Hall WA, Paulson E, et al. Correlation of ADC with pathological treatment response for radiation therapy of pancreatic cancer. *Transl Oncol.* 2018;11(2):391–8.
 35. Liu Y, Bai R, Sun H, Liu H, Wang D. Diffusion-weighted magnetic resonance imaging of uterine cervical cancer. *J Comput Assist Tomogr.* 2009;33(6):858–62.
 36. Brandão AC, Lehman CD, Partridge SC. Breast magnetic resonance imaging: diffusion-weighted imaging. *Magn Reson Imaging Clin N Am.* 2013;21(2):321–36.
 37. Heo SH, Jeong YY, Shin SS, Kim JW, Lim HS, Lee JH, et al. Apparent diffusion coefficient value of diffusion-weighted imaging for hepatocellular carcinoma: correlation with the histologic differentiation and the expression of vascular endothelial growth factor. *Korean J Radiol.* 2010;11(3):295–303.
 38. Surov A, Eger KI, Potratz J, Gottschling S, Wienke A, Jechorek D. Apparent diffusion coefficient correlates with different histopathological features in several intrahepatic tumors. *Eur Radiol.* 2023;33(9):5955–64.
 39. Schob S, Meyer J, Gawlitz M, Frydrychowicz C, Müller W, Preuss M, et al. Diffusion-weighted MRI reflects proliferative activity in primary CNS lymphoma. *PLoS ONE.* 2016;11(8):e0161386.
 40. Surov A, Hamerla G, Meyer HJ, Winter K, Schob S, Fiedler E. Whole lesion histogram analysis of meningiomas derived from ADC values. Correlation with several cellularity parameters, proliferation index Ki 67, nucleic content, and membrane permeability. *Magn Reson Imaging.* 2018;51:158–62.
 41. Surov A, Chang YW, Li L, Martincich L, Partridge SC, Kim JY, Wienke A. Apparent diffusion coefficient cannot predict molecular subtype and lymph node metastases in invasive breast cancer: a multicenter analysis. *BMC Cancer.* 2019;19(1):1043.
 42. Surov A, Clauser P, Chang YW, Li L, Martincich L, Partridge SC, et al. Can diffusion-weighted imaging predict tumor grade and expression of Ki-67 in breast cancer? A multicenter analysis. *Breast Cancer Res.* 2018;20(1):58.
 43. Guo C, Chen X, Xiao W, Wang Q, Sun K, Wang Z. Pancreatic neuroendocrine neoplasms at magnetic resonance imaging: comparison between grade 3 and grade 1/2 tumors. *Onco Targets Ther.* 2017;10:1465–74.
 44. Ma C, Yang P, Li J, Bian Y, Wang L, Lu J. Pancreatic adenocarcinoma: variability in measurements of tumor size among computed tomography, magnetic resonance imaging, and pathologic specimens. *Abdom Radiol (NY).* 2020;45(3):782–8.
 45. Bian Y, Jiang H, Cao K, Mms XF, Li J, Ma C, et al. The relationship between microscopic tumor size and CT tumor size in pancreatic ductal adenocarcinoma. *Clin Imaging.* 2021;76:30–7.
 46. Yang P, Mao K, Gao Y, Wang Z, Wang J, Chen Y, et al. Tumor size measurements of pancreatic cancer with neoadjuvant therapy based on RECIST guidelines: is MRI as effective as CT? *Cancer Imaging.* 2023;23(1):8.
 47. Bilreiro C, Andrade L, Marques RM, Matos C. Diffusion-weighted imaging for determining response to neoadjuvant therapy in pancreatic cancer: a systematic review and meta-analysis. *Eur Radiol.* 2024;34(5):3238–48.
 48. Tang L, Zhou XJ. Diffusion MRI of cancer: from low to high b-values. *J Magn Reson Imaging.* 2019;49(1):23–40.
 49. Ma C, Liu L, Li J, Wang L, Chen LG, Zhang Y, et al. Apparent diffusion coefficient (ADC) measurements in pancreatic adenocarcinoma: a preliminary study of the effect of region of interest on ADC values and interobserver variability. *J Magn Reson Imaging.* 2016;43(2):407–13.
 50. Ma C, Guo X, Liu L, Zhan Q, Li J, Zhu C, et al. Effect of region of interest size on ADC measurements in pancreatic adenocarcinoma. *Cancer Imaging.* 2017;17(1):13.

Publisher's note

Springer Nature remains neutral with regard to jurisdictional claims in published maps and institutional affiliations.